Design and Performance Analysis of a Novel PM Assisted Synchronous Reluctance Machine

Shaopeng Wang[1, 2], Jinguang Ma[1,2], Chengcheng Liu[1,2], Youhua Wang[1,2], Gang Lei[3], Youguang Guo[3] and Jianguo Zhu[4]

1 State Key Laboratory of Reliability and Intelligence of Electrical Equipment (School of Electrical Engineering, Hebei University of Technology), Tianjin 300130, China

2 Province-Ministry Joint Key Laboratory of EFEAR, Tianjin 300130, China)

3 School of Electrical and Data Engineering, University of Technology Sydney, Sydney, NSW, Australia

4 School of Electrical and Information Engineering, University of Sydney, NSW, Sydney, Australia

Correspondence: 2016020@hebut.edu.cn; Tel.: 13752694973

Current address: Hebei University of Technology, No. 8, Guangrong Road, Hongqiao District, Tianjin, 300130, China.

These authors contributed equally to this work.

Abstract: This paper proposes a novel permanent magnet assisted synchronous reluctance (PMAREL) machine, the main structure of this machine is quite similar to that of traditional PMAREL machine, and the main difference is that the grain-oriented silicon steel is used to replace some part of the stator teeth. The rolling direction of the grain-oriented silicon steel is along the radial direction of the machine, thus the advantage of higher permeability and higher kneel point in this material can be used to release the flux saturation problem of the traditional non-grain-oriented steel used in the PMAREL machine when the applied current density is high. Firstly, the structure of both proposed novel and traditional PMAREL machines are optimized and the design parameters are determined. Secondly the electromagnetic and mechanical performance are compared in these two machines which includes the demagnetization analysis, mechanical stress analysis when the rotor at the maximum speed, torque ability, efficiency by using the finite element method (FEM). It can be seen that the problem of stator teeth saturation in the novel PMAREL has been alleviated, and compared with the traditional PMAREL machine, the novel PMAREL has higher efficiency, wider speed range and 7% higher torque ability.

Keywords: Permanent magnet assisted synchronous reluctance (PMAREL) machine, grain-oriented silicon steel, optimization, finite element method (FEM).

0. Introduction

By using high co-energy permanent magnet (PM) to produce the magnetic field, PM machine can have the benefits of high output torque ability, high efficiency and power density, thus the PM machines have been widely used in various energy conversion appliances [1-4]. However, the price of rare earth PMs increases and fluctuates greatly in recent years. Therefore, reducing the material cost in PM machines

has become a trend and the no-rare earth or less rare earth PM concept are proposed for the machine design.

Among these concepts increasing the proportion of reluctance torque in the total torque, and adopting low-cost ferrite to produce the magnetic field is a good method [5-9].

To improve the reluctance torque, the key is to increase the saliency ratio and using the grain-oriented silicon steel is a good way. In [10], A new synchronous reluctance machine (NSynRM) is proposed in this paper, it is designed with the grain-oriented steel inserted into the part of magnetic barrier of rotor core, where the rolling direction of the grain-oriented steel sheets are along the d-axis direction and the stacking direction of that are along the q-axis direction, thus the saliency ratio of this machine has been improved. In [11], a new rotor for synchronous reluctance machine is proposed, each pole of rotor core is made by the grain-oriented silicon steel sheets stacked with its rolling direction along the d-axis direction and the shear direction along the q-axial direction. The experiment results show that the saliency ratio and the torque ability of this machine is very high. In [12], a flux switching permanent magnet machine with grain-oriented steel core is proposed, the simulation results show that its torque has been improved 20% higher than that of the traditional flux switching machine.

When the maximum current density is applied, the stator teeth of PMAREL machine will be partially saturated. Therefore, a novel stator structure of PMAREL machine is proposed to solve this problem, the main structure of this machine is quite similar to the traditional PMAREL machine, and the main difference is that the grain-oriented silicon steel is used to replace some part of the stator teeth. The rolling direction of the grain-oriented silicon steel is along the radial direction of the machine, thus the advantage of higher permeability and higher kneel point in this material can be used to release the flux saturation problem. By using the finite element method (FEM), the mechanical and electromagnetic properties of novel PMAREL and traditional PMAREL have been optimized and compared.

1. Topology of Traditional and Novel PMAREL Machine

Fig. 1 shows the topology of traditional and novel PMAREL machine, where only 1/6 model are illustrated. It can be seen that these two machines are both designed with 36 stator slots and 6 rotor poles. For the mechanical robustness, both the outside and inside iron ribs are designed and only two magnetic barrier layers are designed. In these two machines, the adjacent magnetic barriers are parallel to each other, the width of the barrier where to put the PM is wider as the ferrite magnet is used to produce the PM magnetic field. There is no difference between these two machines on the rotor side, however the detailed dimension will be different after the design optimization. For the stator side, the distributed winding configuration is used, and the main difference is that the grain-oriented silicon steel is used to replace some part on the stator teeth in the novel PMAREL machine, as shown in Fig. 1(b).

Table I tabulates the basic parameters of the traditional and novel PMAREL machine. In the design optimization process for these two machines, these basic parameters are kept not changed.

2. Design and Optimization

The main parameters for design optimization of traditional and novel PMAREL machine are shown

in Fig. 2, it can be seen that there are 5 main parameters in the traditional PMAREL machine and 8 main parameters in the novel PMAREL machine as the enrollment of grain-oriented silicon steel in the stator teeth. During the design optimization process the bellow parameters are confined as follows,

$$\begin{gathered} 6\text{mm} \le H_1 \le 9\text{mm} \\ 2.5\text{mm} \le W_1 \le 4.5\text{mm} \\ 45\text{deg} \le \theta \le 49\text{deg} \\ 8\text{mm} \le W_2 \le 11\text{mm} \\ 11\text{mm} \le W_3 \le 15\text{mm} \end{gathered} \tag{1}$$

$$\begin{gathered} L_1 = 1\text{mm} \\ 16\text{mm} \le L_2 \le 20\text{mm} \\ 1\text{mm} \le L_3 \le 4\text{mm} \end{gathered} \tag{2}$$

The average torque and torque ripple are settled for the optimization target based on the FEM method. The optimization results have been illustrated in Fig. 3. As shown, for achieving higher average torque, the torque ripple will be increased as well, and the Pareto front line have been obtained. It can be seen that with the adoption of grain-oriented silicon steel in the novel PMAREL machine, its average torque will be higher and the torque ripple will be lower than the traditional PMAREL machine. Thus, the enrollment of the grain-oriented silicon steel in the PMAREL is valuable. For the overall consideration of the torque ripple and average torque, the optimization parameters of these two machines are determined as tabulated in Table II. It can be seen that the lower L1 and L3 the better the performance of the novel PMAREL machine as the ratio of grain-oriented silicon steel in the stator teeth is improved, and for the mechanical robustness consideration, the minimum value of the above two parameters are determined to equal 1 mm.

3. Demagnetization Analysis

As the ferrite magnet is used to produce the magnetic field in the PMAREL machine, when the machine is under the high load situation and moreover when the excited current density is very high, then the ferrite magnet will face the risk of demagnetization. In this section the demagnetization situation of the ferrite magnet in PMAREL machine with different current density is analyzed. The demagnetization curve of the ferrite magnet is shown in Fig. 4. When the flux density inside the PM is lower than the knee point, then the PM will have the risk of irreversible demagnetization. For the ferrite magnets used in this study, irreversible demagnetization occurs when the PM internal flux density less than 0.15 T. Fig. 5 shows the flux density in the ferrite magnet along the magnetization direction with different current density by using FEM. It can be seen that the maximum flux density appears on the upper surface of first layer PM. Therefore, irreversible demagnetization is more likely to occur in the first layer PM and the flux density of the PM is lower when the current density is higher. The minimum internal flux density of PM is 0.27 T at rated current density (7 A/mm^2), which has enough margin compared with demagnetization point. And the minimum internal flux density of PM is 0.2 T at the max current density of 14A/mm^2, thus the ferrite magnet can work safely.

4. Stress analysis

As the rotor structure in these two machines are the same, and for the performance improvement, wide magnetic barrier in the rotor core is designed. Then the rotor core will face the problem of safety operation especially at the high speed. In this section the rotor stress is analyzed by using ANSYS WORKBENH platform. Table III tabulates the main mechanical properties of the materials used for rotor core. Fig. 6 shows the mechanical stress and deformation distribution of the rotor cores at the maximum rotation speed (6000 rpm). As shown, the maximum stress is appeared on the shaft part due to the shaft takes the role of rotating the whole rotor and also the stress located on the magnetic rib is high as these parts are worked to keep the rotor as a whole part. The maximum deformation is appeared on the out part of rotor side. It can be seen that the mechanical stress and deformation of rotor core are still within the acceptable range. Therefore, the rotor can be operated with good state at maximum speed.

5. Electromagnetic Performance Comparison

In this section, the electromagnetic performances of the novel PMAREL machine are investigated and compared with the traditional PMAREL machine.

Fig. 7(a) shows the magnetization curve of the non-oriented silicon steel sheets, it can be seen that the kneel point of this material is about 1.4 T, Fig. 7(b) and Fig. 7(c) shows the magnetization curve of the grain-oriented silicon steel sheets along the rolling direction and the shear direction respectively. It can be seen that their kneel points are 1.9 T and 1.2 T respectively. Fig. 7(d) and Fig. 7(e) shows the magnetic flux density distribution. It can be seen that the magnetic flux density on the stator teeth in the traditional machine is saturated and the maximum flux density is about 1.8 T. For the novel machine, the magnetic flux density is about 1.6 T, and the flux density on the grain-oriented silicon steel sheets is very high and it close to 2.1 T, which is resulted by high permeability characteristic of the used material. The inside rib and outside rib are both saturated for these two machines.

Fig. 8 shows the PM flux linkage waveform and induced voltage waveform of tradition and novel PMAREL machines. For ease of comparison, only the A phase PM flux linkage and the induced voltage waveforms are shown. It can be seen that the addition of grain-oriented silicon steel has no effect on the waveform and show good sinusoidal properties. Because it is under no load, the flux density of the magnetic core is low, so there is no obvious difference between the amplitude of the two machines.

The average torque and torque ripple of PMAREL machine can be expressed by,

$$T_{ave} = \frac{3}{2}P\left(\lambda_{PM} i_q + \left(L_d - L_q\right) i_d i_q\right) \tag{3}$$

$$T_{ripple} = \frac{T_{P\_P}}{T_{ave}} \times 100\% \tag{4}$$

where P is the number of pole pairs, L_d the d-axis inductance, L_q the q-axis inductance, i_d the d-axis current, i_q the q-axis current, λ the PM flux linkage, T_{ave} is the average torque, $T_{P\text{-}P}$ is the peak-to-peak value of torque, T_{ripple} is the torque ripple.

Fig. 9 shows the torque waveform and the torque with the variation of current density of traditional and novel PMAREL machine. In Fig. 9, ICD and IICD means the current density for the traditional and novel PMAREL respectively, and the unit is A/mm^2. For achieving maximum torque, there is a determined current angle for the different current density. In PMAREL, the optimal current angle is

between 50 deg and 55 deg. As shown, the novel PMAREL has higher torque ability especially when the current density increases. When current density is 14 A/mm^2, the torque for novel and traditional PMAREL machine is 24.1 Nm, and 22.3 Nm respectively, and the torque increase rate is about 8%, and torque ripple is quite similar.

The torque increase rate is defined by:

$$T_k = \frac{T_n - T_t}{T_t} \times 100\% \quad (5)$$

where T_n, T_t is the average torque of the traditional and novel PMAREL machine respectively.

Fig. 10 shows the efficiency map of traditional and novel PMAREL machine under the determined voltage of 100V. It can be seen that the maximum torque of the traditional PMAREL is lower than that of the novel PMAREL machine. For the novel PMAREL, torque drop point appears at 3200 rpm. Therefore, the constant torque operation region of the novel PMAREL machine is about 6.7% wider than that of the traditional PMAREL machine which is resulted by the adopted grain-oriented silicon steel release the flux saturation in the stator teeth. The main efficiency of these two machines is quite similar and the efficiency has reached to 87% in the constant torque region and for the constant power region the efficiency has reached to about 95%.

6. Conclusion

With enrolling of the grain-oriented silicon steel sheets, a novel PMAREL machine is proposed in this paper. By using the FEM, a novel PMAREL and a benchmark traditional PMAREL are both designed, optimized, analyzed and compared, some conclusions have been obtained:

1) The saturation of stator teeth can be released by adding the grain-oriented silicon steel in the teeth with the rolling direction along the radial direction of the machine.

2) For the stress analysis at the maximum speed, these two PMAREL machines have similar stress distribution and the maximum stress is appeared at the shaft part, and the maximum stress is far less than the maximum allowable tensile strength, thus the PMAREL machines can be operated at the maximum speed.

3) The maximum average torque has been improved about 8%, the torque ripple basically remains the same and the constant torque operation region has been improved about 6.7% in the novel PMAREL, as the adopted grain-oriented silicon steel has very good electromagnetic performance in the rolling direction.

Reference

[1] A. M. EL-Refaie et al., "Advanced High-Power-Density Interior Permanent Magnet Motor for Traction Applications," *IEEE Trans. Ind.* Appl., vol. 50, no. 5, pp. 3235-3248, 2014.

[2] C. Liu et al., "Performance Evaluation of an Axial Flux Claw Pole Machine With Soft Magnetic Composite Cores," *IEEE Trans. Appl. Supercond.,* vol. 28, no. 3, pp. 1-5, April 2018.

[3] X. Sun, Z. Shi, G. Lei, Y. Guo, and J. Zhu, "Multi-objective design optimization of an IPMSM based on

multilevel strategy," *IEEE Trans. Ind. Electron*., vol. 68, no. 1, pp. 139-148, Jan. 2021.

[4] C. Liu, S. Wang, Y. Wang, G. Lei, Y. Guo and J. Zhu, "Development of a new flux switching transverse flux machine with the ability of linear motion," in *CES Transactions on Electrical Machines and Systems*, vol. 2, no. 4, pp. 384-391, Dec. 2018.

[5] X. Sun et al., "Study on segmented rotor switched reluctance motors with different rotor pole numbers for BSG system of hybrid electric vehicles," *IEEE Trans. Veh. Technol,* vol. 28, no. 6, pp. 5537-5547, Jun. 2019.

[6] X. Sun et al., "Analysis and design optimization of a permanent magnet synchronous motor for a campus patrol electric vehicle," *IEEE Trans. Veh. Technol,* vol. 68, no. 11, pp. 10535-10544, Nov. 2019.

[7] W. Zhao, F. Xing, X. Wang, T. A. Lipo and B. Kwon, "Design and Analysis of a Novel PM-Assisted Synchronous Reluctance Machine with Axially Integrated Magnets by the Finite-Element Method," *IEEE Trans. Magn.,* vol. 53, no. 6, pp. 1-4, 2017.

[8] H. Cai, B. Guan and L. Xu, "Low-Cost Ferrite PM-Assisted Synchronous Reluctance Machine for Electric Vehicles," *IEEE Trans.Ind. Electron.*,vol. 61, no. 10, pp. 5741-5748, 2014.

[9] Z. Q. Zhu, W. Q. Chu and Y. Guan, "Quantitative comparison of electromagnetic performance of electrical machines for HEVs/EVs," in *CES Transactions on Electrical Machines and Systems*, vol. 1, no. 1, pp. 37-47, 2017.

[10] S.P.Wang, J.G.Ma, C.C.Liu et al., "Design and Performance Analysis of a Novel Synchronous Reluctance Machine," *International Journal of Applied Electromagnetics and Mechanics*, vol. 63, no. 2, pp.249-265, 2020.

[11] S. Taghavi and P. Pillay, "A Novel Grain-Oriented Lamination Rotor Core Assembly for a Synchronous Reluctance Traction Motor with a Reduced Torque Ripple Algorithm," *IEEE Trans. Ind. Appl.,* vol. 52, no. 5, pp. 3729-3738, 2016.

[12] J. Ma et al., "Optimal Design of an Axial-Flux Switched Reluctance Motor with Grain-Oriented Electrical Steel," *IEEE Trans. Ind. Appl.,* vol. 53, no. 6, pp. 5327-5337, 2017.

Tab.1

Basic parameters of 36-slot/6-pole machines

Parameters	Value	Unit
Stator outer diameter	140	mm
Rotor outer diameter	80	mm
Stack length	63	mm
Air gap length	1	mm
Inside rib length	0.8	mm
Outside rib length	0.5	mm
Slot fill factor	55	%
Maximum Current density	14	A/mm^2
Rated Current density	7	A/mm^2
DC voltage	100	V
PM remanence	0.4	T

Tab.2

Optimization results of key parameters

Parameters	Model I	Model II	Unit
H_1	8.5	8	mm
H_2	3	5	mm
H_3	5	5	mm
W_1	4.1	3.8	mm
W_2	11.6	10	mm
W_3	12.2	13.6	mm
θ	45.7	46	deg
L_1	-	1	mm
L_2	-	18	mm
L_3	-	1	mm

Tab.3

Mechanical properties of materials

Parameter	Density(kg/m^3)	Young's Modulus (Gpa)	Poisson's ratio	Tensile strength (Mpa)
Silicon steel	7750	220	0.30	300
PM	7600	120	0.24	80

Fig.1 Topology of (a) traditional and (b) novel PMAREL machine

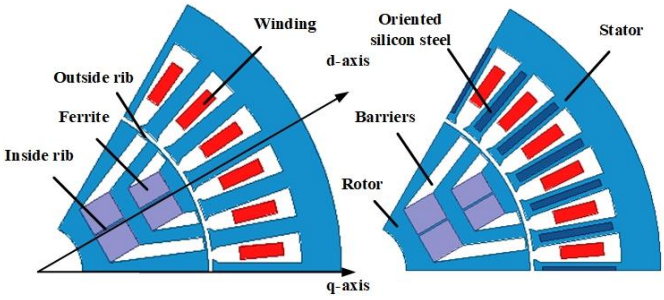

(a) (b)

Fig.2 Main parameters for design optimization of (a) traditional and (b) novel PMAREL machine

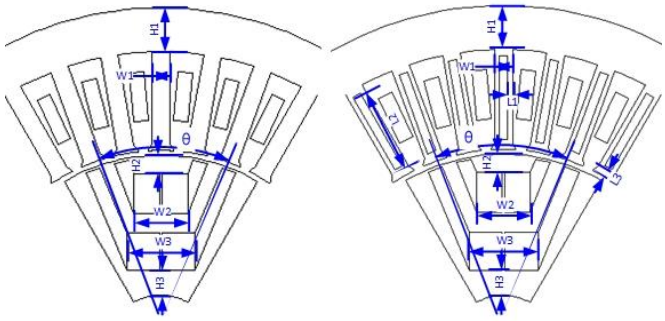

(a) (b)

Fig.3 Optimization results of average torque and torque ripple.(a) traditional and (b) novel PMAREL machine

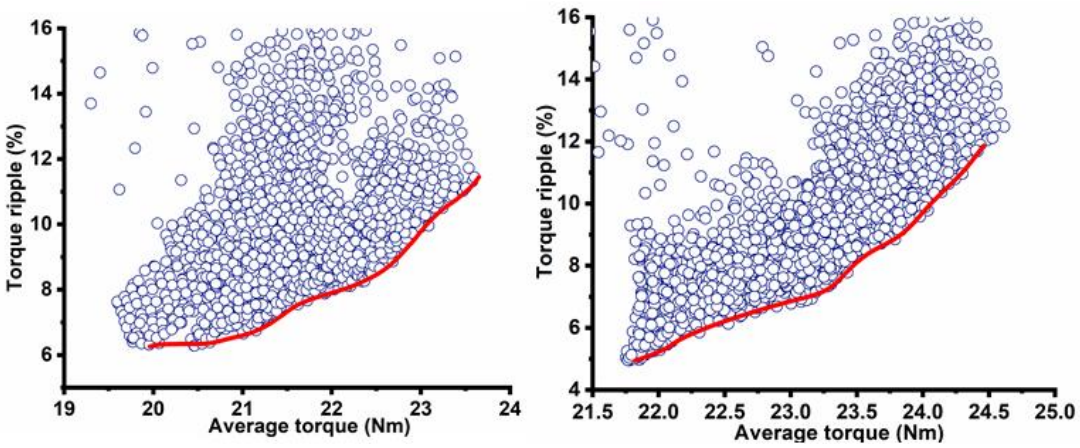

(a) (b)

Fig.4 Demagnetization curve

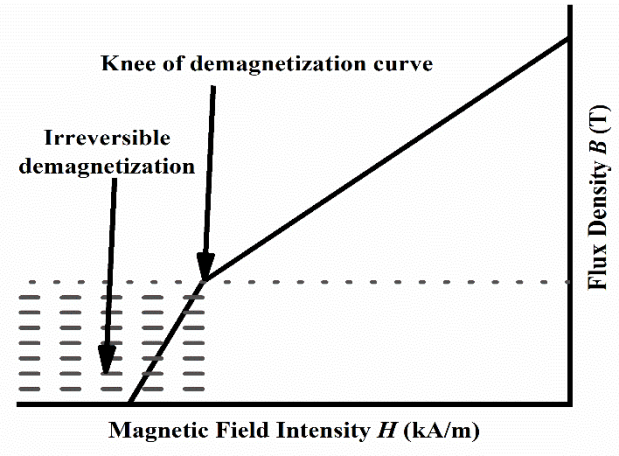

Fig.5 Flux density of rotor. (a) Current density of 7A/mm^2,(b) Current density of 14A/mm^2.

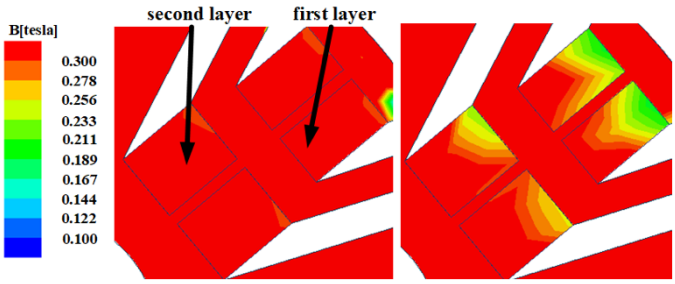

(a) (b)

Fig.6 Mechanical stress and deformation distributions. (a) Mechanical stress. (b)Mechanical deformation.

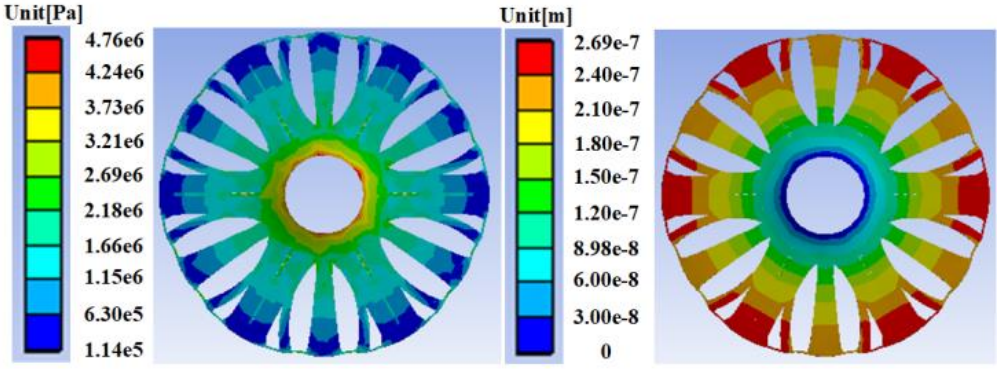

(a) (b)

Fig.7 Flux density map of rotor fed by 14 A/mm^2 current density, (a) B-H curve for non-grain-oriented silicon steel, (b) B-H curve for grain-oriented silicon steel along the stacking direction, (c) B-H curve for grain-oriented silicon steel along the shear direction, flux density distribution of (d) traditional and (e) novel PMAREL machine

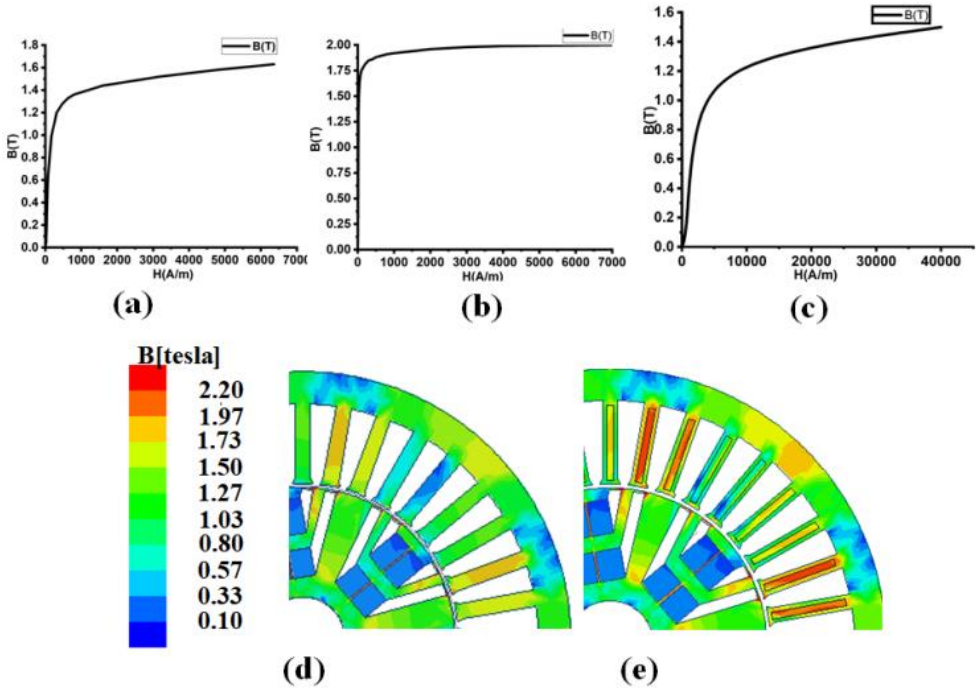

Fig.8 (a) Flux linkage waveform, (b) Induced voltage waveform

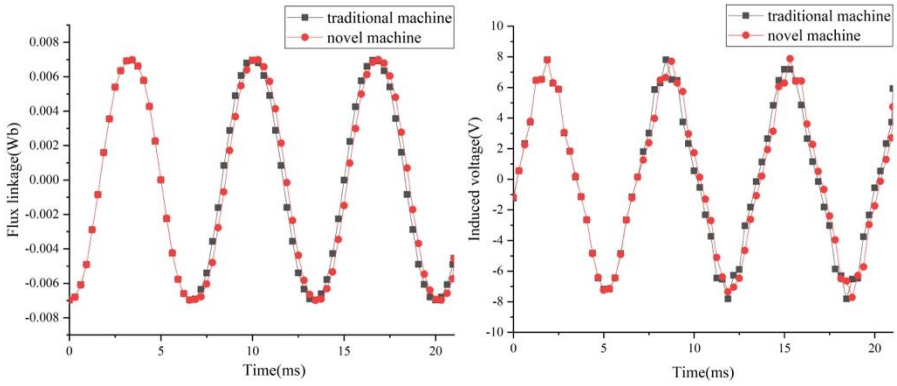

(a) (b)

Fig.9 Torque versus current. (a) torque waveform, (b) torque versus current density and current angle

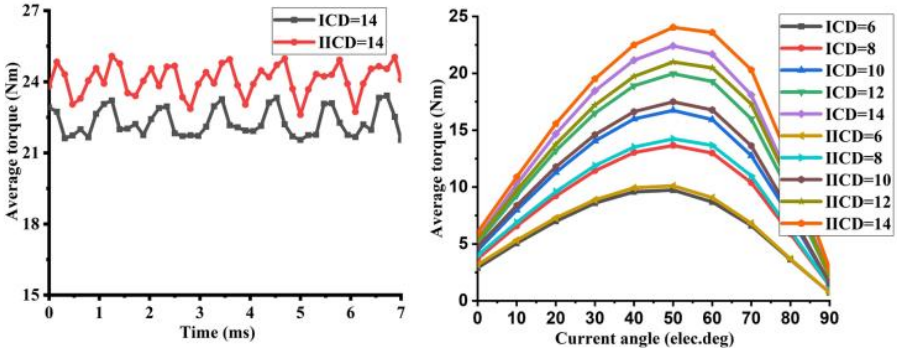

(a) (b)

Fig.10 Efficiency map for (a) traditional PMAREL machine and (b) novel PMAREL machine

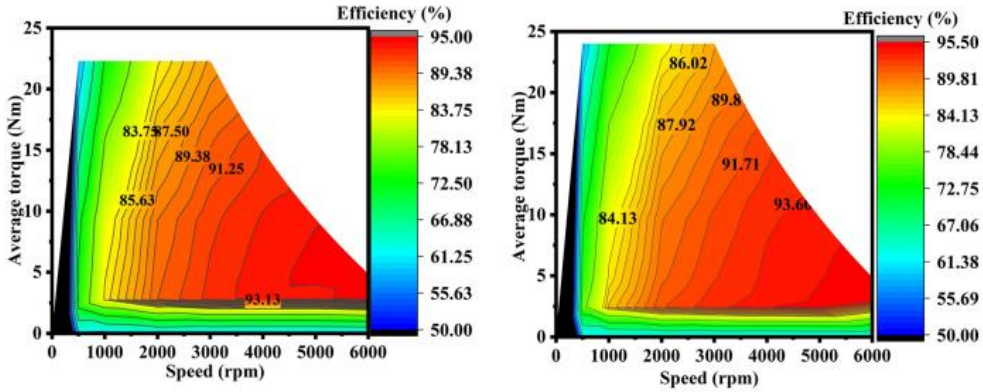

(a) (b)